Electrochimica Acta 166 (2015) 277–284

Contents lists available at ScienceDirect

Electrochimica Acta

journal homepage: www.elsevier.com/locate/electacta

Improved stability of electrochromic devices using Ti-doped V_2O_5 film

Youxiu Wei, Junling Zhou, Jianming Zheng, Chunye Xu *

CAS Key Laboratory of Soft Matter Chemistry, Department of Polymer Science and Engineering, Hefei National Laboratory for Physical Science at the Microscale, University of Science and Technology of China, Hefei 230026, PR China

ARTICLE INFO

Article history:
Received 14 January 2015
Received in revised form 11 March 2015
Accepted 12 March 2015
Available online 16 March 2015

Keywords:
electrochromic device
titanium-doped vanadium oxide
memory effect
stability

ABSTRACT

Vanadium pentoxide (V_2O_5) is a promising material for constructing electrochromic devices, due to its outstanding properties of lithium ion intercalation/deintercalation. However, its poor cyclic stability limits practical applications. We report here that V_2O_5 films gain significantly improved cyclic stability by doping with titanium (Ti) and perform well in WO_3-based electrochromic devices. V_2O_5 films were fabricated by spin coating with a vanadium triisopropoxy oxide solution followed by heat treatment. X-ray diffraction studies reveal that introducing the Ti element reduces the crystallinity of a V_2O_5 film and distorts its layer structure. The cyclic stability of the V_2O_5 films increases as the doped Ti content increases. The electrochromic device assembled with an optimized V_2O_5 electrode (V:Ti = 2:1) has lasted 200,000 cyclic switching times between the lowest (2%) and highest (62%) transmittance with no significant degradation of performance.

1. Introduction

Amorphous V_2O_5 has been widely investigated because of its interesting electrochemical performance. It has been known to intercalate large amounts of lithium ions, making it especially useful for battery and electrochromic applications [1–5]. A typical electrochromic device (ECD) includes two transparent substrates that sandwich five functional layers, including a transparent conductive layer, an electrochromic layer, an electrolyte layer, an ion storage layer, and another transparent conductive layer. ECDs can change their optical properties between different colors, which could lead to substantial energy savings. V_2O_5 has been studied extensively as a counter electrode material in ECDs, where it provides electrochemical oxidation and reduction reactions that balance charge transfer at the electrochromic working electrode during optical switching; it exhibits a minor color change during the insertion and extraction of ions as described in our previous work [6]. The typical electrochromic reaction of V_2O_5 in a lithium perchlorate ($LiClO_4$) electrolyte can be written as follows:

$$V_2O_5 + xLi^+ + xe^- = Li_xV_2O_5 \quad (1)$$

However, reports about its intrinsic electrochromic properties are very limited, due to several disadvantages arising from its low conductivity, poor cyclic reversibility, and lack of stability [7–9].

Much of the recent research has focused on the synthesis and fabrication of nanostructure V_2O_5 to improve its electrochromic properties. Nanostructure could offer larger charge capacity and higher diffusion coefficient of Li ions by means of high specific surface area and short diffusion distance. Recently, Yan [10] and Wei et al. [11] reported the nanostructure V_2O_5 exhibited high current density due to the larger specific surface area. However, nanostructured films still suffer from unsatisfactory cyclic stability. Furthermore, doping transition metal ions has been studied to improve ion intercalation properties. Several studies have reported that the electrochemical properties of V_2O_5 can be improved progressively by doping metal ions into its matrix, such as Mn, Cu, Zn and Ag [8,12–15]. The effect of Ti on the reversibility of Li^+ insertion into vanadium-based materials is also of particular interest [16–19]. Ozer et al. [20] and Lee et al. [21] observed that a proper amount of Ti addition could improve the cyclic stability and charge capacity of V_2O_5. Ti doped V_2O_5 films have been always prepared using sol–gel synthesis, which offers the advantages of low cost and sample equipment. However, the precipitation usually occurred at high doped Ti content during the sol–gel process.

In this research, we obtained the clear doped solution for overcoming the problem and prepared smooth doped V_2O_5 films with different Ti contents through the spin coating method. The addition of Ti provided excellent reversibility due to the distorted V_2O_5 layer structure, which was investigated by the X-ray

* Corresponding author at: CAS Key Laboratory of Soft Matter Chemistry, Department of Polymer Science and Engineering, Hefei National Laboratory for Physical Science at the Microscale, University of Science and Technology of China, Hefei 230026, PR China. Tel.: +86 551 6360 3459; fax: +86 551 6360 3459.
E-mail address: chunye@ustc.edu.cn (C. Xu).

http://dx.doi.org/10.1016/j.electacta.2015.03.087
0013-4686/

diffraction (XRD). There were less reports about the inorganic ECD based on the sol-gel derived Ti–V_2O_5 films. We first prepared inorganic ECD with 200,000 cycle life using improved Ti–V_2O_5 films as counter electrode and WO_3 films as working electrode. To our best knowledge, it is longest life time for inorganic ECD based on V_2O_5. This device regulated transmittance well in the infrared region and had good memory effect.

2. Experiment

2.1. Chemicals and accessories

All reagents were chemically pure and used without purification. We used vanadium triisopropoxy oxide [$VO(OC_3H_7)_3$] and titanium isopropoxide [$Ti(OC_3H_7)_4$], purchased from TCI (Tokyo, Japan), for the Ti-doped film. Tungsten powder (W) and 30% hydrogen peroxide (H_2O_2) were used to prepare the electrodeposition solution for the WO_3 films. $LiClO_4$ was used to prepare the electrolyte. We used indium tin oxide (ITO) glass with an area of 3.5 cm × 3.5 cm for the preparation of the electrochromic electrodes.

2.2. Preparation of Ti-doped V_2O_5 films

The Ti-doped V_2O_5 coating solutions were synthesized by controlled hydrolytic polycondensation of the $VO(OC_3H_7)_3$ and titanium $Ti(OC_3H_7)_4$ [19]. $VO(OC_3H_7)_3$ and $Ti(OC_3H_7)_4$ were dissolved into the isopropanol separately to obtain a transparent solution with a molar concentration of 0.14 M. Then the Ti solution was added to the vanadium solution during the stirring process. The high doped concentration can easily generate precipitation in the mixed solution, we dropped appropriate volume acetic acid into the mixed solution. After an hour, a clear and stable faint yellow solution was obtained for preparing films. The solutions with different V:Ti molar ratios (5:1, 4:1, 3:1, 2:1 and 1:1) were prepared by mixing solutions with different volume ratios.

The compound Ti-doped V_2O_5 films were prepared by spin coating on ITO glass, using the WS-400BZ-8NPP-LITE (Laurell Technologies Corp., North Wales, PA, USA). Spin coating was performed in air so that the ambient moisture would partially hydrolyze the alkoxide film. Film with a thickness of about 50 nm was obtained by using a spin rate of 1000 rpm for 30 seconds. The coatings were uniform, transparent, hard and stable after firing at a temperature of 300 °C for 30 minutes. Annealing at a high temperature could cause the phase separation of TiO_2 from V_2O_5 [16].

2.3. Deposition of WO_3 films

WO_3 precursor sol was prepared by the wet chemical synthetic route. Colorless and turbid peroxopolytungstic acid (PPTA) was prepared by mixing W metal powder (6 g) and hydrogen peroxide (H_2O_2, 30%, 60 mL) at room temperature [22,23]. In our experiment, PPTA solution was ultrasonicated to remove excess H_2O_2 and became clear after filtration. Subsequently, the PPTA solution was continuously refluxed, first at 55 °C for 6 hours, then 65 °C for 1 hour and finally at 85 °C for 30 minutes in order to remove excess H_2O_2 and gel the solution. The refluxing time was precisely controlled to avoid precipitation during gelation process. Equal volume of ethanol was added to the sol immediately after the gelation process. Finally, the mixture turned into a deep yellow deposition sol after refluxing at 50 °C for 12 hours. The final product was a transparent, orange-colored PPTA sol. The sol remained stable at a low temperature and was used as an electroplating solution.

WO_3 films were electrodeposited in a three-electrode cell (CHI650D, CH Instruments, Shanghai, China) with a platinum (Pt) sheet as a counter electrode, a silver wire as a reference electrode and ITO glass (3.5 cm × 3.5 cm) as a working electrode. A constant cathodic potential of −0.5 V was applied to the ITO glass in the prepared electroplating solution. Dark blue WO_3 film was obtained and then dried in air after washing it with ethanol. The colorless and transparent WO_3 films were obtained after heat treatment at 300 °C for 30 minutes.

2.4. Preparation of electrochromic device

We chose 1 M $LiClO_4$/PC solution as the electrolyte. Ti-doped V_2O_5 film and WO_3 film were used as the counter electrode and working electrode, respectively. Ultraviolet (UV)-curable sealant was smeared along the edge of one electrode, and one injection port was left. Then another electrode was pressed on it, leaving a gap of 100 μm. After the sealant was solidified using UV light irradiation, the electrolyte was injected through the injection port into the gap between the two electrodes. Finally, the injection port was sealed using UV-curable sealant.

2.5. Characterization of the films and devices

The structure of the films was investigated by XRD on a diffractometer with Cu Kα (Kα = 1.5418 Å, 40 kV, 200 mA) radiation (TTR-III, Rigaku, Japan). The chemical states and compositions of the Ti-doped V_2O_5 films were analyzed by XPS (ESCALAB 250, Thermo-VG Scientific, East Grinsted, West Sussex, UK). XPS spectra were recorded using Al–Kα radiation (1486.6 eV) as the excitation source. The surface morphology of the films was examined using scanning electron microscopy (SEM; Sirion 200, FEI, Hillsboro, Oregon, USA). The spectroelectrochemical properties of films and devices were investigated from the results obtained using a UV/visible/near-infrared spectrophotometer (V-670; JASCO, Tokyo, Japan) and electrochemical analyzer (CHI 650D; CH Instruments, Shanghai, China). The electrochemical properties were tested in a three-electrode cell. We used a Pt sheet as the counter electrode and a silver wire as the reference electrode; the liquid electrolyte was 0.1 M $LiClO_4$/PC.

Table 1
Binding energy and full-width at half-maximum (FWHM) of the O1s, $V2p_{3/2}$, $Tip_{3/2}$ peaks for the Ti-doped V_2O_5 films with different concentrations of Ti components.

V:Ti	Binding energy (eV)								
	O1s				$V2p_{3/2}$				
	A	FWHM	B	FWHM	A	FWHM	B	FWHM	V^{4+}/V^{5+}
1:0	530.59	1.38	531.97	2.29	514.75	1.08	516.57	1.5	7.23%
5:1	530.54	1.15	532.11	1.41	517.83	1.3	516.62	1.41	49.35%
4:1	530.57	1.15	532.09	1.49	517.88	1.25	516.69	1.4	50.71%
3:1	530.6	1.18	532.04	1.69	517.88	1.22	516.67	1.42	52.65%
2:1	530.67	1.13	532.13	1.46	517.9	1.23	516.8	1.62	51.72%
1:1	530.53	1.15	532.04	1.55	517.72	1.02	–	–	–

3. Results and discussion

3.1. Property of films

3.1.1. XPS analysis of Ti-doped V_2O_5 films

All of Ti-doped V_2O_5 films were examined by XPS. The regional XPS spectra were all calibrated with the binding energy of the adventitious C1s peak (284.79 eV). We chose doped films with a 2:1 (V:Ti) molar ratio as examples for the analysis of the chemical states of V and O. Other molar ratios of doped films have similar characteristics. A typical survey spectrum (Fig. A. 1 shown in the supporting information) for a doped V_2O_5 film with a 2:1 (V:Ti) molar ration shows two intense peaks of C1s and N1s. Nitrogen may originate from the surface contamination. The main C1s peak at 284.79 eV is assigned to hydrocarbon and the isopropanol used as a solvent in the solution [24]. Table 1 summarizes the binding energy and full-width at half maximum (FWHM) of the O1s and $V2p_{3/2}$ peaks for doped V_2O_5 films with different concentrations of Ti.

Fig. 1b shows the high resolution O1s and V2p core-level spectra of the doped V_2O_5 films with a 2:1 (V:Ti) molar ratio. The $V2p_{3/2}$ peak can be described as the sum of two components centered at 517.9 eV (A) and 516.8 eV (B), which are related to the two oxidation states V^{5+} and V^{4+}. Compared with the pure V_2O_5 film shown in Fig. 1a, the addition of Ti increases the proportion of V^{4+} in films. Table 1 presents the proportion percentage of V^{4+}/V^{5+} in Ti-doped films with different ratios. The proportion of V^{4+} does not vary obviously when the concentrations of Ti are increased. The oxygen signal at 530.59 eV and 530.67 eV in Fig. 1a and b correspond to the oxygen ions of the oxide layer, and the additional oxygen components at 532.13 eV and 531.97 eV can be ascribed to C-O bonds originating from isopropanol solvent or other surface contamination [24]. The two peaks in the Ti2p XPS spectra (Fig. A. 2 shown in the supporting information) at about 459.1 eV and 464.75 eV are assigned to $Ti2p_{3/2}$ and $Ti2p_{1/2}$, respectively, indicating that Ti^{4+} exists in the oxidized state. The intensity of the peaks increases with the Ti content. The XPS results above indicate that Ti-doped V_2O_5 films mainly contain mixed oxides of V^{5+}, V^{4+} and Ti^{4+}.

3.1.2. Structural characterizations of films

XRD studies were performed on the annealed Ti-doped V_2O_5 films to investigate the influence of Ti doping on the structure. Fig. 2 shows the XRD patterns of Ti-doped V_2O_5 films with different molar ratios (a) and WO_3 films on ITO glass (b).

As shown in Fig. 2a, the peaks are indexed following the standard pattern [JCPDS file no. 41-1426 and no. 27-0940]. The XRD data show the existence of V_2O_5 and V_3O_7 in the film. The peaks corresponding to V_3O_7 only exist in pure V_2O_5 films and is of low crystallinity. As our work is mainly focused on the layer structure change of V_2O_5 by adding Ti content. In addition, if we consider the V^{4+}/V^{5+} ratio, we could obtain the ratio from the XPS data (Fig. 1a and Table 1), the content of V_3O_7 is little. We do not discuss much about V_3O_7. In our case, as shown in Fig. 2a, V_2O_5 material is basically amorphous and has the typical layer structure, the diffraction peaks correspond to (001) and (002) planes of the interlayer structure. In addition, peaks related to TiO_2 are not observed in Ti-doped V_2O_5 films, indicating that TiO_2 phase is

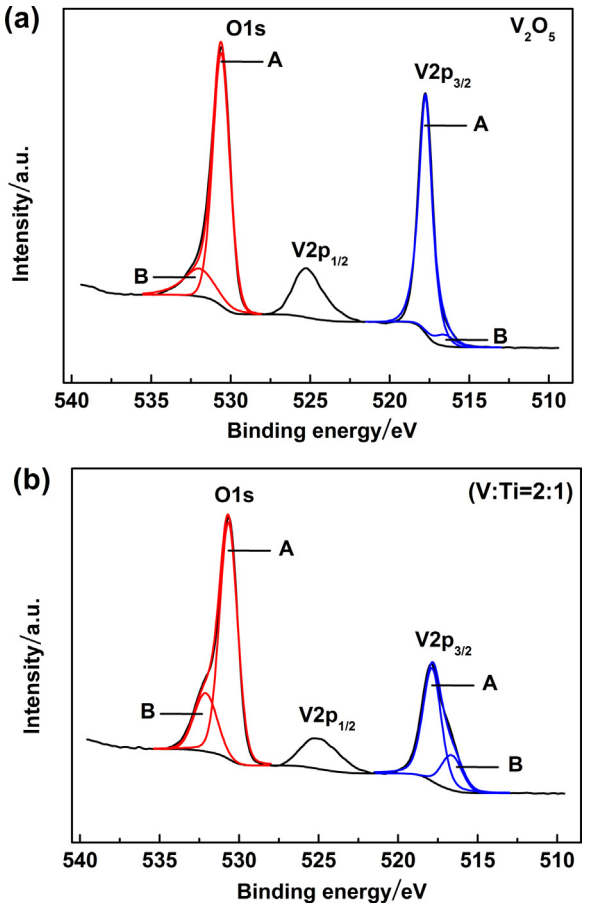

Fig. 1. XPS spectra of O1s and V2p energy regions of pure V_2O_5 film (a) and Ti-doped V_2O_5 films with a 2:1 (V:Ti) molar ratio (b).

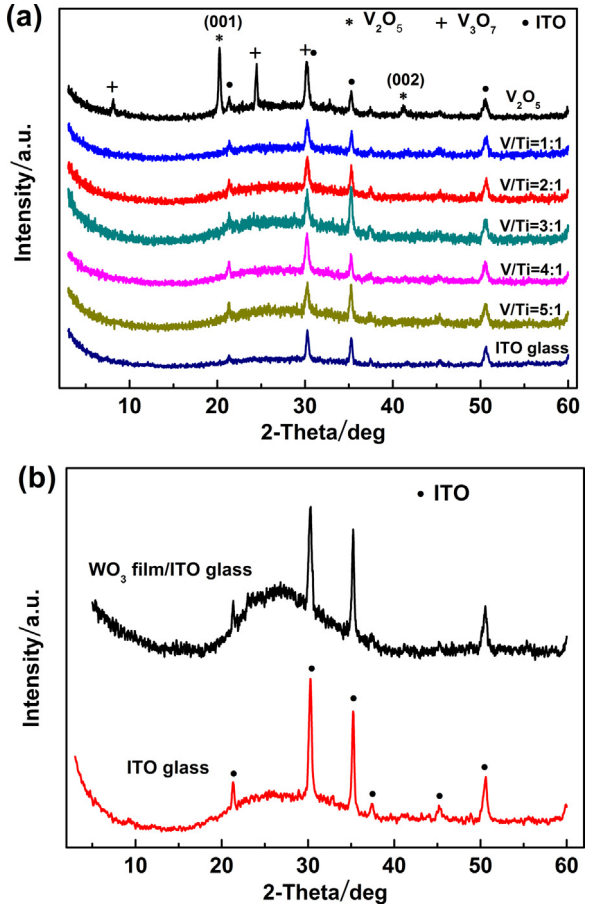

Fig. 2. The XRD patterns of Ti-doped V_2O_5 films with different Ti concentrations (a) and WO_3 film (b) on ITO glass.

amorphous or Ti would incorporate into the structure of V_2O_5. With Ti doping, the diffraction peaks of (001) and (002) planes disappear, which illustrates the layer structure of V_2O_5 is disordered by large amount of Ti doping. Moreover, The XPS data shows that the addition of Ti reduces the valence state of V and increases $V^{4\pm}$ /$V^{5\pm}$ ratio in Ti-doped films. The formation of V–O–Ti bond [16,17] in the interlayer structure could distort layer structure and reduce the valence state of V. In conclusion, Ti incorporates into the structure of V_2O_5 and could render a freer and open V_2O_5 interlayer structure, which could be convenient for Li^+ insertion and extraction process.

WO_3 films also show the amorphous structure with no obvious diffraction peaks. The electrochromic performance of WO_3 films is closely related to their crystallinity. Amorphous WO_3 films have faster response time and a higher coloration efficiency than crystalline films. We have verified that the crystal WO_3 films do not reach the bleached state from the colored state as easily as amorphous films, which could impair the optical performance of the ECD.

3.1.3. Surface morphology of Ti-doped V_2O_5 films

A SEM study of the surface morphologies and possible morphological changes of Ti-doped V_2O_5 films with different Ti concentrations reveals that, in general, the as-prepared Ti-doped V_2O_5 films have a featureless surface morphology. Fig. 3a shows the rough but not uneven surface of pure V_2O_5 films, which

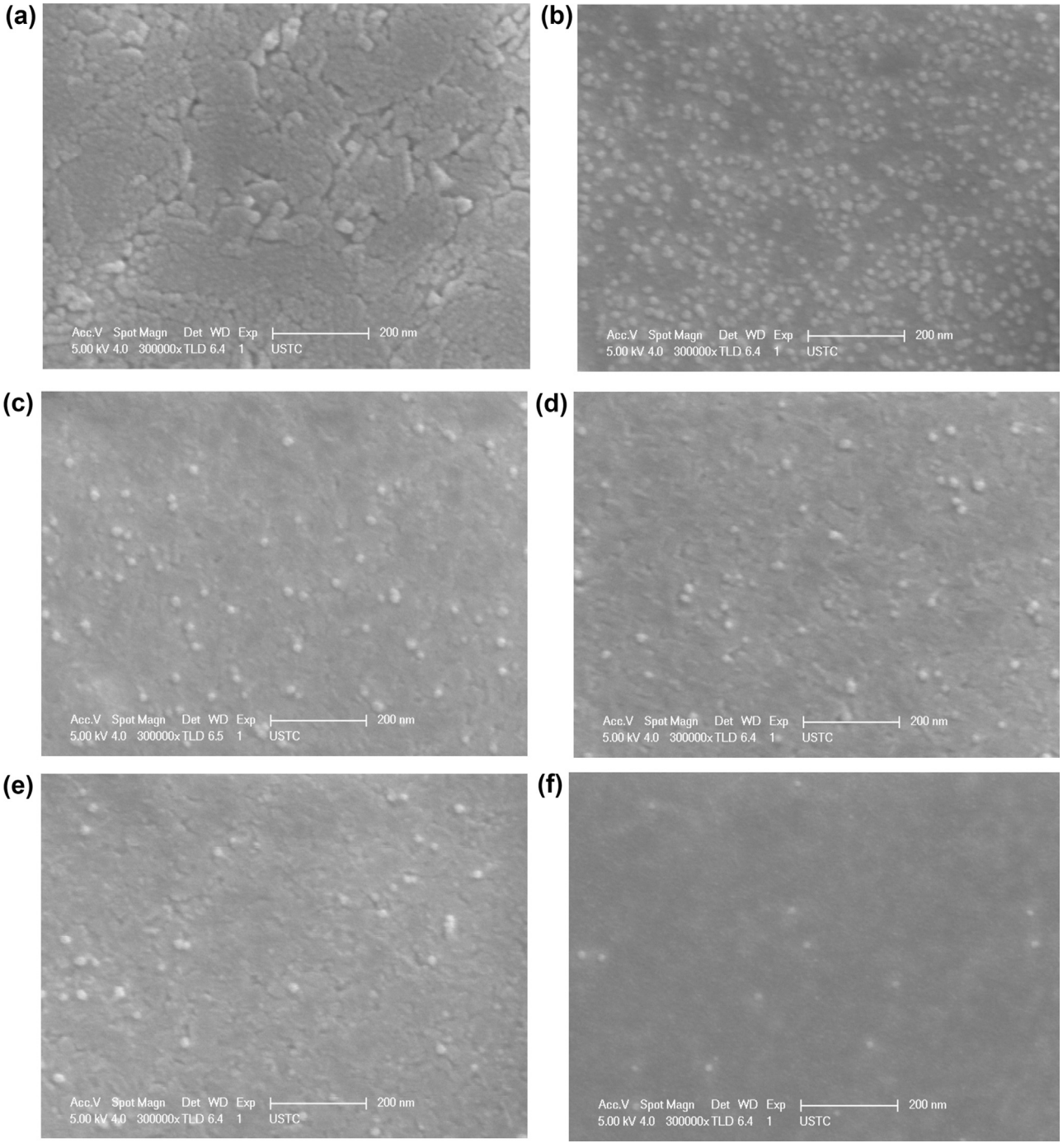

Fig. 3. SEM images of Ti-doped V_2O_5 films with different V/Ti molar ratios: (a) 1:0, (b) 5:1, (c) 4:1, (d) 3:1, (e) 2:1 and (f) 1:1.

comprise dozens of nanometers sized nanoparticles. Small V_2O_5 colloidal particles were formed by the hydrolysis-polycondensation of vanadium alkoxide, the subsequent heating treatment removed the solvent to obtain V_2O_5 particle, which also led to the crack on the surface of V_2O_5 films. These nanoparticles provide efficient contact with the electrolyte solution. However, with the increasing Ti content, the grain boundary become blurry and disappeared. The Ti-doped films become smoother and more compacted than pure V_2O_5 films, thereby decreasing their surface area. Li diffusion within the material is slower and more difficult than in a liquid electrolyte or along the grain boundary. That factor may explain the smaller charge capacity of highly Ti-doped V_2O_5 films compared to pure V_2O_5 films during the initial charge/discharge cycles.

3.1.4. Electrochemical and optical properties of films

To study the effects of Ti doping on the electrochemical characteristics of V_2O_5 films, we carried out cyclic voltammetry (CV) measurements of Ti-doped V_2O_5 films. Fig. 4a shows the plot of current density versus applied voltage at a 20 mV/s sweep rate. The CV curve of the pure V_2O_5 film shows two cathodic reduction peaks (−0.28 V, −0.52 V), attributable to Li^+ intercalation, and two anodic peaks (−0.035 V, 0.17 V), which correspond to Li^+ extraction. With increases in Ti content, the two anodic and two cathodic peaks broaden and merge to form one peak. Compared with pure V_2O_5 film, the current density decreases as Ti content increases, because of the compacted surface topography and the reduced amount of active V_2O_5 content. In addition, the addition of Ti reduces the anodic voltage and Li ions can leave the structure easily, which could improve the cyclic stability of these films.

Films were subjected to repeated insertion and release cycles to determine their cyclic performance. The result, shown in Fig. 4b, indicates that the capacity density of pure V_2O_5 decreases sharply after hundreds of cycles. For doped V_2O_5 films, the cyclic stability gradually improves as Ti content increases. The addition of Ti in the molar ratios V:Ti = 1:1 and 2:1 dramatically improves the cyclic stability of the films. This is because that the Ti content distorts the layer structure of V_2O_5 and makes more free space for the Li^+ intercalation/deintercalation process, resulting in the excellent cyclic stability. Therefore, we used the molar ratios V:Ti = 1:1 and 2:1 to prepare stable counter electrodes.

The optical transmittance spectra of as-prepared films in the oxidized and reduced states are shown in Fig. 5. The data show that, as the doped Ti content rises, the transmittance of films tends to increase in the visible region and to decrease in the infrared region. The improved transmittance of Ti-doped V_2O_5 films over pure V_2O_5 films is greater in the reduced state than the oxidized state, which can improve the bleached transmittance of the ECD. When V:Ti = 1:1, the transparency declined due to the increasing haze of highly doped films. The haze value measured 0.8% and 17.5% for films at V:Ti = 2:1 and 1:1, respectively. Considering the stability and high transmittance, we chose V:Ti = 2:1 as the best ratio for ECD counter electrodes.

Assessing the optimum thickness for the WO_3 film requires taking coloration efficiency (*CE*) into consideration. This term is defined as the change in the optical density ($\triangle OD$) per unit of electrode area (A) at a given wavelength, which can be characterized in the following equation [25].

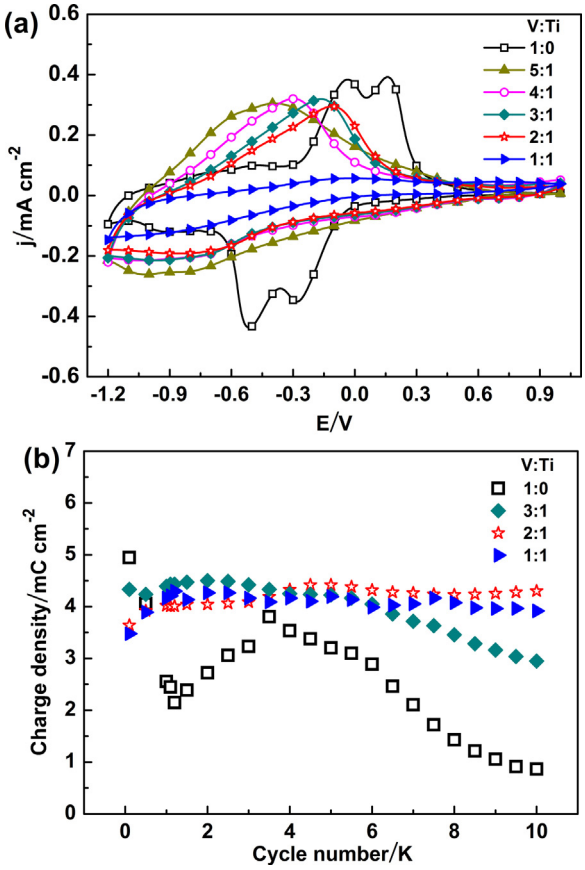

Fig. 4. Cyclic voltammogram at a 20 mV/s sweep rate (a) and stability (b) of Ti-doped V_2O_5 films with different Ti concentrations.

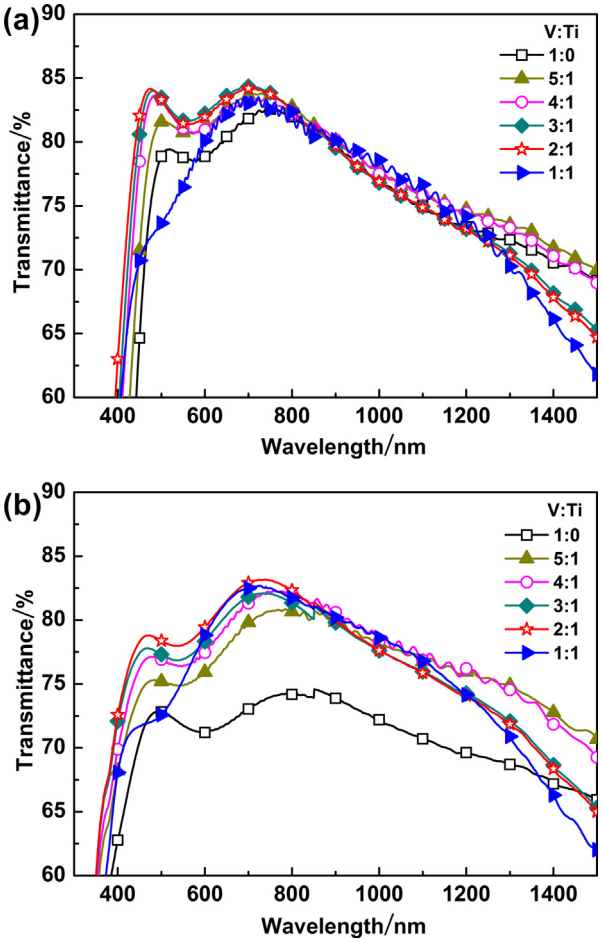

Fig. 5. The transmittance of Ti-doped V_2O_5 films with different Ti levels in oxidation (a) and reduction states (b).

$$CE = \Delta OD/(q/A) = \log(T^b/T^c)/(q/A) \quad (2)$$

Where q is the inserted charge capacity, and T^b and T^c are the transmittances of the bleached and colored states, respectively.

The transmittance modulation was defined as:

$$\Delta\%T = T^b - T^c \quad (3)$$

T^b and T^c represent the light transmittance of a certain wavelength in the bleached and colored states, respectively.

Fig. 6a presents the CE value of WO_3 as a function of film thickness. We selected the wavelength of 580 nm as the testing wavelength. The CE data form a parabolic curve with the variation of thickness. Little difference of CE value exists in the range of 400 to 800 nm thickness and the value is approximately 30 to 35 cm^2/C. In our case, WO_3 films with a 400 nm thickness were chosen for the fabrication of the ECD working electrode. As shown in Fig. 6b, the transmittance of bleached WO_3/ITO glass reaches over 85% in the visible region. The Δ%T reaches 80% in the infrared region.

3.2. Stability and memory effect of ECDs

3.2.1. Stability at room temperature, 25 °C

Fig. 7 shows the optical transmittance along with photographs of ECD (3.5 cm × 3.5 cm) in the bleached and colored states. The device changes between bleached state (the solid line) and colored state (the dotted line) by applying ± 1.5 V voltage. The transmittance of the device in the bleached state exhibits transmittance of about 62% at 900 nm; in the colored state, it achieves a low transmittance (less than 2%). Clearly, the colored device has low transmittance in the infrared region, reducing heat transport, which could be also used for infrared modulation.

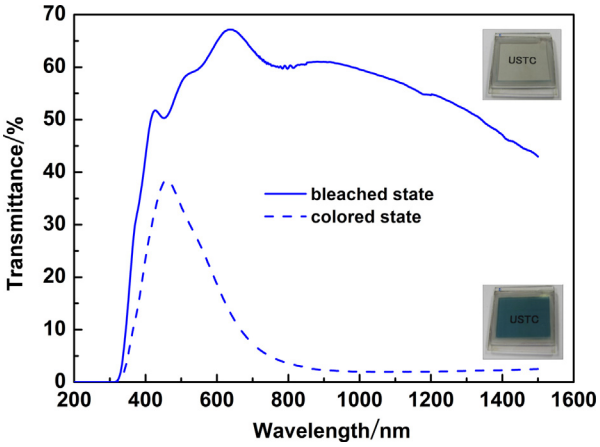

Fig. 7. The optical transmittance, with photographs of 3.5 cm × 3.5 cm ECD.

We conducted a long-term switching test to investigate the electrochromic stability of the device and show the results in Fig. 8. Each electrochromic cycle was obtained by applying a voltage of ±1.5 V. Changes in the charge density with the cycle number is plotted in Fig. 8a. The inserted charge density and the extracted charge density are basically the same, indicating good reversible performance of the device. Fig. 8b shows the transmittance change during continuous cycling of an ECD at the 680 nm and 900 nm

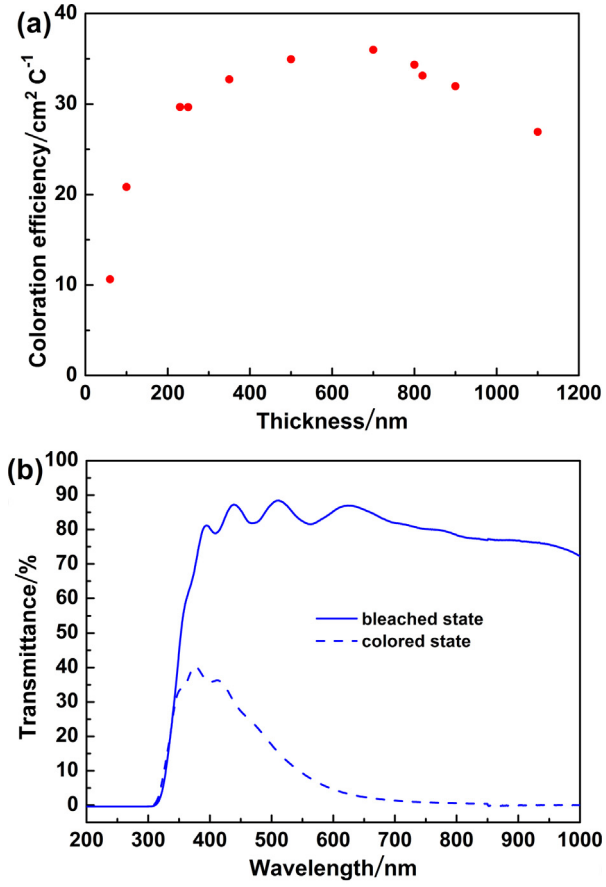

Fig. 6. The coloration efficiency (a) at the 580 nm wavelength and the transmittance (b) of WO_3 films.

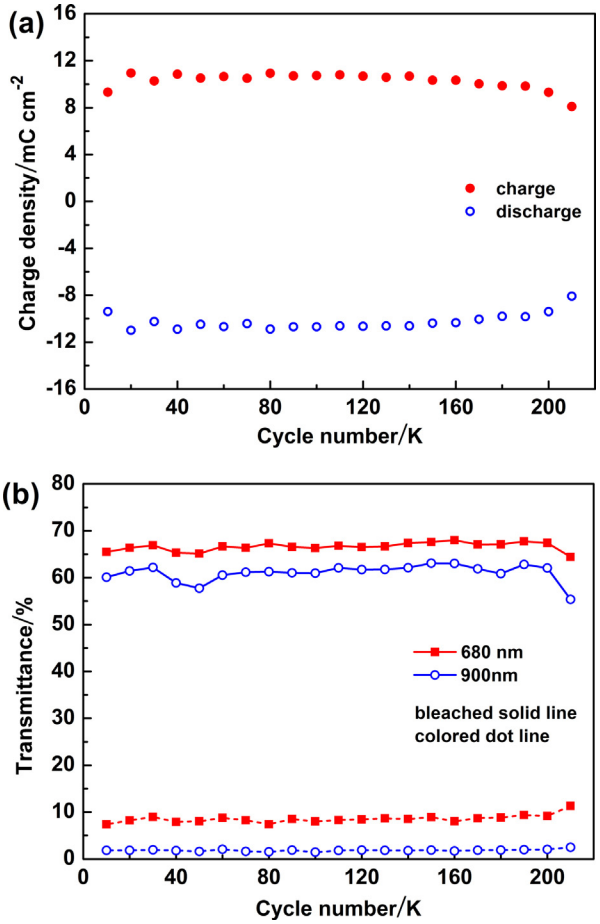

Fig. 8. Charge density (a) and transmittance (b) variation curves of ECD with the cycle number. K: 1000.

wavelengths. The Δ%T could reach 60% in the near-infrared region. Both of the charge density and transmittance of the device remain stable through 200,000 cycles, which is a longest lifetime inorganic ECD based on V_2O_5, to our best knowledge. This device exhibits excellent cyclic stability at room temperature.

3.2.2. Stability at high temperature, 60 °C

Fig. 9 shows the transmittance of ECD during switching at a higher temperature of 60 °C. As we all know, the overall charge depends mostly on the charge capacity of counter electrode, as WO_3 film has a very high charge capacity. However, at high temperature, the balance of charge capacity between counter and working electrodes is a very important factor affecting cyclic stability of an ECD based on our experiments. As for this purpose, we prepared the Ti-doped V_2O_5 film and WO_3 film having approximate charge capacity before assembling. Then we can see from Fig. 9, the device is stable for tens of thousands of cycles test. After 60,000 switching cycles, the transmittance data decrease a little at both 680 nm and 900 nm wavelengths. However it is still insufficient for practical application. So for matching the capacity of WO_3 in high temperature, maintaining stable and higher transmittance contrast, we have done the research on the electrolyte and obtained some valuable progress. More experiment is going on in our lab for solving this problem.

3.2.3. Memory effect

The term "memory effect" is used to describe the ability of an ECD to retain its set color state after voltage is removed from the device. We kept the ECD in its bleached or colored state without external voltage, then recorded its transmittance change. The curve in Fig. 10 shows the relationship between transmittance and time. As time passed, the transmittance at 680 nm and 900 nm is almost the same in both bleached and colored state. As shown in the figure, the transmittance just shifts upward with less than 5% change over seven days. This result indicates the ECD we prepared performs good memory effect.

4. Conclusion

We used spin coating method to obtain uniform Ti-doped V_2O_5 compound films. Our XRD data demonstrated that the addition of high concentrations of Ti distorted the layer structure of the films and reduced the degree of crystallinity, providing more free space for Li^+ intercalation and deintercalation. The addition of Ti resulted in increased transmittance and improved stability during cyclic switching. An ECD was prepared by using Ti-doped V_2O_5 film with the optimized molar ratio (V:Ti = 2:1) as the counter electrode and WO_3 film as the working electrode. The device proved excellent reversibility up to 200,000 cycles at room temperature, good optical contrast of 60% in the infrared region, and good memory effect for about seven days.

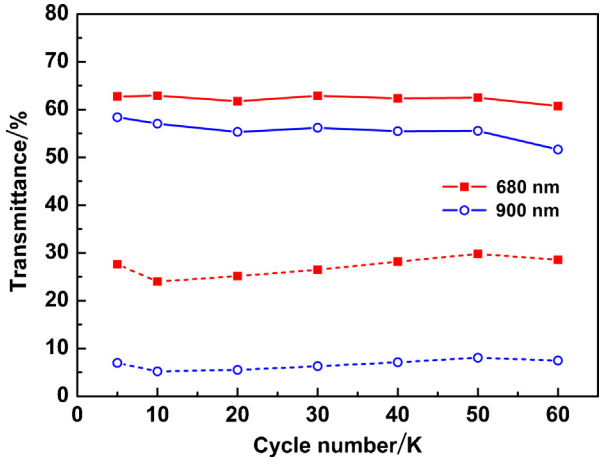

Fig. 9. The transmittance variation of the ECD at 680 nm and 900 nm, with cycle number, at 60 °C. In the figure, solid line indicates the bleached state, dot line represents the colored state.

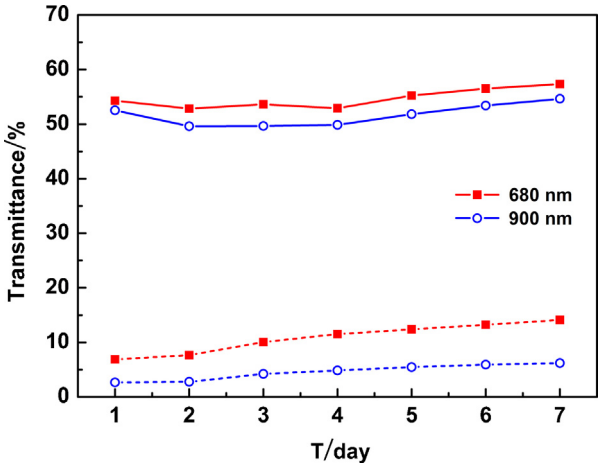

Fig. 10. Electrochromic memory function of the ECD at 680 nm and 900 nm in the bleached (solid line) and colored states (dotted line).

Acknowledgments

This work received financial support from the National Natural Science Foundation of China (21273207,21274138 and 21474096); the "Hundred Talents Program" of CAS.

Appendix A. Supplementary data

Supplementary data associated with this article can be found, in the online version, at http://dx.doi.org/10.1016/j.electacta.2015.03.087.

References

[1] S. Kim, M. Taya, C. Xu, Contrast, Switching Speed, and Durability of V_2O_5–TiO_2 Film-Based Electrochromic Windows, J. Electrochem. Soc. 156 (2009) E40.
[2] S. Kim, M. Taya, Electrochromic windows based on V_2O_5–TiO_2 and poly (3,3-dimethyl-3,4-dihydro-2H-thieno[3,4-b][1,4]dioxepine) coatings, Sol. Energy Mater. Sol. Cells 107 (2012) 225.
[3] Q. Du, S. Mi, J. Zheng, C. Xu, A comparative study of the electrochemical behavior of complementary polymer electrochromic devices based on different counter-electrodes, Smart Mater. Struct. 22 (2013) 125025.
[4] S.N. Alamri, A.A. Joraid, Smart windows with different thicknesses of V_2O_5 as ion storage layers, in: Y.M. Huang (Ed.), Optoelectronic Materials, Pts 1 and 2, Trans Tech Publications Ltd, Stafa-Zurich, 2010 p. 743.
[5] Q. Du, Y.X. Wei, J. Zheng, C. Xu, Donor-(-bridge-acceptor type polymeric materials with pendant electron-withdrawing groups for electrochromic applications, Electrochim. Acta 132 (2014) 258.
[6] Y.X. Wei, M. Li, J. Zheng, C. Xu, Structural characterization and electrical and optical properties of V_2O_5 films prepared via ultrasonic spraying, Thin Solid Films 534 (2013) 446.
[7] S.H. Lee, H.M. Cheong, P. Liu, C.E. Tracy, Improving the Durability of Amorphous Vanadium Oxide Thin-Film Electrode in a Liquid Electrolyte, Electrochem. Solid-State Lett. 6 (2003) A102.
[8] D.M. Yu, S.T. Zhang, D.W. Liu, X.Y. Zhou, S.H. Xie, Q.F. Zhang, Y.Y. Liu, G.Z. Cao, Effect of manganese doping on Li–ion intercalation properties of V_2O_5 films, J. Mater. Chem. 20 (2010) 10841.
[9] S.J. Yoo, J.W. Lim, B. Choi, Y.E. Sung, Enhanced Reliability of Electrochromic Devices with a LiPON Protective Layer, J. Electrochem. Soc. 154 (2007) P6.
[10] X. Rui, Z. Lu, Z. Yin, D.H. Sim, N. Xiao, T.M. Lim, H.H. Hng, H. Zhang, Q. Yan, Oriented molecular attachments through sol–gel chemistry for synthesis of ultrathin hydrated vanadium pentoxide nanosheets and their applications, Small 9 (2013) 716.
[11] D. Wei, M.R.J. Scherer, C. Bower, P. Andrew, T. Ryhaenen, U. Steiner, A Nanostructured Electrochromic Supercapacitor, Nano Letters 12 (2012) 1857.

[12] F. Coustier, J. Hil, B.B. Owens, S. Passerini, W.H. Smyrl, Doped Vanadium Oxides as Host Materials for Lithium Intercalation, J. Electrochem. Soc. 146 (1999) 1355.
[13] M. Giorgetti, M. Berrettoni, Doped V_2O_5-Based Cathode Materials: Where Does the Doping Metal Go? An X-ray Absorption Spectroscopy Study, Chem. Mater. 19 (2007) 5991.
[14] F. Coustier, S. Passerini, W.H. Smyrl, Dip-coated silver-doped V_2O_5 xerogels as host materials for lithium, Solid State Ionics 100 (1997) 247.
[15] H. Park, Manganese vanadium oxides as cathodes for lithium batteries, Solid State Ionics 176 (2005) 307.
[16] A. Šurca, S. Benčič, B. Orel, B. Pihlar, Spectroelectrochemical studies of V/Ti-, V/Ti/Zr- and V/Ti/Ce-oxide counter-electrode films, Electrochim. Acta 44 (1999) 3075.
[17] M.B. Sahana, C. Sudakar, C. Thapa, V.M. Naik, G.W. Auner, R. Naik, K.R. Padmanabhan, The effect of titanium on the lithium intercalation capacity of V_2O_5 thin films, Thin Solid Films 517 (2009) 6642.
[18] S. Tian, A. Xing, H. Tang, Z.H. Bao, G.M. Wu, Enhanced cycling stability of TiO_2-coated V_2O_5 nanorods through a surface sol–gel process for lithium ion battery applications, J. Mater. Chem. A 2 (2014) 2896.
[19] A. Davies, R.J. Hobson, M.J. Hudson, W.J. Macklinb, R.J. Neat, Sol-gel-derived vanadium and titanium oxides as cathode materials in high-temperature lithium polymer-electrolyte cells, J. Mater. Chem. 6 (1996) 49.
[20] N. Özer, S. Sabuncu, J. Cronin, Electrochromic properties of sol-gel deposited Ti-doped vanadium oxide film, Thin Solid Films 338 (1999) 201.
[21] K. Lee, G.Z. Cao, Enhancement of Intercalation Properties of V_2O_5 Film by TiO_2 Addition, J. Phys. Chem. B 109 (2005) 11880.
[22] M. Deepa, A.K. Srivastava, T.K. Saxena, S.A. Agnihotry, Annealing induced microstructural evolution of electrodeposited electrochromic tungsten oxide films, Appl. Surf. Sci. 252 (2005) 1568.
[23] A.J. More, R.S. Patil, D.S. Dalavi, S.S. Mali, C.K. Hong, M.G. Gang, J.H. Kim, P.S. Patil, Electrodeposition of nano-granular tungsten oxide thin films for smart window application, Mater. Lett. 134 (2014) 298.
[24] J. Świątowska-Mrowiecka, V. Maurice, S. Zanna, L. Klein, P. Marcus, XPS study of Li ion intercalation in V_2O_5 thin films prepared by thermal oxidation of vanadium metal, Electrochim. Acta 52 (2007) 5644.
[25] L.C. Chen, K.C. Ho, Design equations for complementary electrochromic devices: application to the tungsten oxide–Prussian blue system, Electrochim. Acta 46 (2001) 2151.